ORIGINAL ARTICLE

Nanoscale optical parametric amplification through super-nonlinearity induction

Özüm Emre Aşırım[1] · **Mustafa Kuzuoğlu**[2]

Abstract
Optical parametric amplification (OPA) is a nonlinear process through which a low-power input wave is amplified by extracting energy from an interaction medium that is energized by a high-intensity pump wave. For a significant amplification of an input wave, a sufficiently long interaction medium is required, which is usually on the order of a few centimeters. Therefore, in the small scale, OPA is considered unfeasible, and this prevents it from being employed in micro and nanoscale devices. There have been recent studies that proposed microscale OPA through the use of micro-resonators. However, there is currently no study that has suggested high-gain nanoscale OPA, which could be quite useful for implementing nanoscale optical devices. This study aims to show that nanoscale OPA is feasible through the concurrent maximization of the pump wave induced electric energy density and the polarization density (nonlinear coupling strength) within the interaction medium, which enables a very high amount of energy to be transferred to the input wave that is sufficient to amplify the input wave with a gain factor that is comparable to those provided by centimeter scale nonlinear crystals. The computational results of our OPA model match with the experimental ones in the context of sum-harmonic generation, which is the wave-mixing process that gives rise to OPA, with an accuracy of 97.6%. The study aims to make room for further investigation of nanoscale OPA through adaptive optics and/or nonlinear programming algorithms for the enhancement of the process.

Keywords Optical parametric amplification · Nonlinear optics · Nanoscale · High energy density

Introduction

Optical parametric amplification (OPA) is the amplification of a low-intensity input wave by a high-intensity pump wave, such that there is an energy transfer from the pump wave-energized interaction medium to the input wave, through which the input wave intensity is increased to a high degree. The main advantage of OPA is that it enables wideband high-gain amplification, as opposed to lasers which offer relatively low gain over a limited bandwidth (Zhang et al. 1993; Lin et al. 2020; Paschotta 2008). Hence, the gain-bandwidth product of optical parametric amplifiers (OPAs) is much higher than lasers. On the other hand, in today's integrated photonic devices, instead of OPAs, lasers are being employed. The reason for this is that OPAs require bulk crystals to yield a significant gain. Most OPAs are based on nonlinear crystals that are at least a few centimeters long (Paschotta 2004; Saleh and Teich 2019). In the micro and nanoscale, OPAs do not offer any measurable gain, as the gain per unit length due to nonlinear coupling is not sufficient to provide a noticeable amplification in such small scales (Saleh and Teich 2019). Hence, micro and nano optical devices are based on light amplification via stimulated emission of radiation (laser) rather than parametric amplification. Inevitably, this limits the performance of integrated photonic devices, as lasers have a narrow operation bandwidth. OPAs on the other hand, would allow tunability over a very large operational bandwidth, while simultaneously offering superior gain compared to lasers. Therefore, it is of high importance to investigate the OPA process in greater depth and to come up with a strategy to employ OPAs in the micro and nanoscale, such that the attained gain over their large bandwidth is comparable to that of lasers.

✉ Özüm Emre Aşırım
ozum.asirim@tum.de

1 Department of Electrical and Computer Engineering, Technical University of Munich, Arcisstrasse 21, 80333 Munich, Germany

2 Department of Electrical and Electronics Engineering, Middle East Technical University, 06800 Ankara, Turkey

OPAs, due to their tunability and large gain-bandwidth product, are quite expensive devices. They are also quite bulky and take up a large space on a laboratory desk (Zhang et al. 2016). They are used for many applications, such as imaging, molecular spectroscopy, inertial confinement fusion, high-energy density physics, chemical sensing, and many others (Zhang et al. 1993; Zhang et al. 2016; Lin et al. 2020; Paschotta 2004; Saleh and Teich 2019; Trovatello et al. 2021; Kuramochi 2021; Baumgartner and Byer 1979). But due to their high-cost and bulkiness, for applications and laboratory measurements requiring high optical-intensity, investigators are often forced to come up with alternative implementations with lower accuracies. For this reason, coming up with an efficient OPA design in the small scale is of great interest for both applicability and for low-cost implementation of a certain experimental process, as in the case of Lab-On-Chip based measurements (Zhang et al. 2016; Trovatello et al. 2021; Kuramochi 2021; Baumgartner and Byer 1979; Marhic et al. 2015; Taghizadeh and Hatami 2017; Valiulis et al. 2008; Fragemann et al. 2003). Therefore, the problem of small-scale OPA has attracted a significant number of researchers in the last decade (Taghizadeh and Hatami 2017; Valiulis et al. 2008; Fragemann et al. 2003; Cholan et al. 2011; Ooi et al. 2017; Aşırım and Yolalmaz 2020; Asırım and Kuzuoglu 2020; Asırım and Kuzuoglu 2020). A growing number of studies have suggested that microscale high-gain OPA is feasible through the implementation of special structural designs (Trovatello et al. 2021; Kuramochi 2021; Baumgartner and Byer 1979; Marhic et al. 2015; Taghizadeh and Hatami 2017; Valiulis et al. 2008; Fragemann et al. 2003; Cholan et al. 2011; Ooi et al. 2017; Aşırım and Yolalmaz 2020; Asırım and Kuzuoglu 2020; Asırım and Kuzuoglu 2020). There are also studies that proposed the use of ultra-nonlinear materials/crystals to decrease the interaction medium length for small-scale OPA realization (Sakhno et al. 2020; Milton et al. 1992; Gonzalez and Lee 2018; Manzoni and Cerullo 2016; Wang et al. 2019; Markov et al. 2018; Ren and Li 2011; Xiao et al. 2021). Most importantly, a recent set of studies has found that small-scale OPA is quite feasible without the use of special structural designs or ultra-nonlinear crystals (Aşırım and Yolalmaz 2020; Asırım and Kuzuoglu 2020; Asırım and Kuzuoglu 2020). These studies have proposed that using just a micro-resonator and an intelligent cavity-design algorithm, an ultra-high gain OPA is possible in the microscale. This study builds upon these latest studies (Aşırım and Yolalmaz 2020; Asırım and Kuzuoglu 2020; Asırım and Kuzuoglu 2020) by eliminating the requirement of a high-Q cavity and goes further to suggest that nanoscale ultra-high gain OPA is also possible, even without the use of a resonator. Here, it is suggested that all that is needed is a smart choice of the pump wave frequency, which concurrently maximizes the interaction medium energy density and the nonlinear

coupling strength (pump wave polarization density). This avoids the challenge of satisfying certain resonator conditions to maintain the imposed resonator dynamics for high-gain OPA operation in the small scale.

Based on the empirical results, it can be deduced that OPA in the micro and nanoscale is impossible to achieve as the interaction medium length is way too short to provide any observable gain (Trovatello et al. 2021; Kuramochi 2021; Baumgartner and Byer 1979; Marhic et al. 2015; Taghizadeh and Hatami 2017; Valiulis et al. 2008; Fragemann et al. 2003; Cholan et al. 2011; Ooi et al. 2017). However, as explained before, the length of the interaction medium is just one factor and there are two other factors, which are the pump wave intensity and the nonlinearity of the interaction medium. Having set the interaction medium length to be in the nanoscale, we will work on the other two to realize OPA at this scale.

During OPA, the electric energy density within an interaction medium is always proportional to the initial pump wave excitation amplitude. The nonlinearity on the other hand, is proportional to the polarization density within the medium that is induced by the pump wave, which couples to the input wave and enables the transfer of energy. The polarization density is correlated with the electric energy density and tends to be high when the electric energy density is high. Hence, we will focus on the concurrent maximization of both the electric energy density and the pump wave induced polarization density, to compensate for the super-short interaction length of the medium. The question is whether such a high electric energy density (and polarization density) can be achieved to observe nanoscale high-gain OPA. As will be shown, it is entirely possible, if one has the knowledge of the dispersion features of an interaction medium and adjusts the pump wave excitation accordingly.

Interestingly, OPA has almost never been investigated through an in-depth dispersion analysis, but rather with frequency-independent nonlinearity coefficients. Although it is true that the 2nd and 3rd order nonlinearity coefficients are mostly constant over the entire IR–Visible–UV range, there can be multiple nonlinearity resonances where extraordinary nonlinear energy coupling is available (Annamalai and Vasilyev 2012; Schmidt et al. 2014; Li et al. 2011; Cheng et al. 2018; Wang et al. 2013; Hanyu Ye et al. 2018; Martinelli, et al. 2001; Varin et al. 2018; Rout et al. 2019; Ceglia et al. 2019; Zygiridis and Kantartzis 2018) due to an abrupt increase in the polarization density, which often leads to a sharp change in the electric energy density and the effective permittivity (Asırım and Kuzuoglu 2020; Boyd 2008). As the energy density and the polarization density are proportional to each other, this study is focused on the simultaneous maximization of both quantities to maximize the energy that is coupled to the input wave, first by condensing the energy density in the interaction medium, and then via

maximizing the coupling of this energy to the input wave. This can compensate for the short length of the medium and enable nanoscale OPA. In the next section, an in-depth investigation on the dispersion features of an interaction medium will be carried out in correspondence with the excitation features of the pump and input waves, to decrypt a given nanoscale interaction medium to function as a reasonably effective parametric amplifier.

Empirical results

In order for OPA to occur at a significant degree for an input wave, usually, at least one of the three conditions need to be satisfied (Saleh and Teich 2019; Taghizadeh and Hatami 2017; Valiulis et al. 2008; Fragemann et al. 2003; Cholan et al. 2011; Ooi et al. 2017; Aşırım and Yolalmaz 2020; Asırım and Kuzuoglu 2020; Asırım and Kuzuoglu 2020; Sakhno et al. 2020; Milton et al. 1992; Gonzalez and Lee 2018; Manzoni and Cerullo 2016; Wang et al. 2019; Markov et al. 2018; Ren and Li 2011; Xiao et al. 2021; Annamalai and Vasilyev 2012): (1) the nonlinearity of the interaction medium should be high. (2) The interaction medium should be sufficiently long (usually in the centimeter scale). (3) The pump wave amplitude is sufficiently high for inducing nonlinear coupling to the input wave. The solution for the intensity gain factor of an input wave after its propagation through an interaction medium of length L, is given by the following semiempirical formula (Saleh and Teich 2019; Boyd 2008)

c: speed of light, ε_0: permittivity of free space, L: medium length, I_{input} : Input wave intensity, ρ: nonlinearity coefficient, n: refractive index, η: intrinsic impedance, ε : Relative permittivity, ω_1 : Angular frequency of the input wave, ω_2 : Angular frequency of the pump wave , E_{pump} : Pump wave electric field amplitude.

The amplitude gain factor is simply expressed as the square root of the intensity gain factor (Fig. 1)

$$G_{Amplitude} = \cosh\left\{\left(L\rho\sqrt{2\omega_1(\omega_2-\omega_1)\eta^3}\sqrt{0.5cn\varepsilon_0E_{pump}^2}\right)\right\}. \tag{2}$$

As shown in Table 1, at the millimeter scale, OPA is extremely weak, even under a high-amplitude pump wave excitation and a relatively high interaction medium nonlinearity. Hence, it can be inferred that at the nanoscale, OPA is totally unfeasible under the assumption of a constant (non-resonant) nonlinearity.

Methods

OPA is a highly frequency dependent process (Aşırım and Yolalmaz 2020; Asırım and Kuzuoglu 2020; Asırım and Kuzuoglu 2020; Sakhno et al. 2020; Milton et al. 1992; Gonzalez and Lee 2018; Manzoni and Cerullo 2016; Wang et al. 2019; Markov et al. 2018; Ren and Li 2011; Xiao et al.

$$\frac{I_{input}(z=L)}{I_{input}(z=0)} = G_{intensity} = \cosh^2\left\{\left(L\rho\sqrt{2\omega_1(\omega_2-\omega_1)\eta^3}\sqrt{0.5cn\varepsilon_0E_{pump}^2}\right)\right\} \tag{1}$$

Fig. 1 OPA through an interaction medium with a nonlinearity coefficient of ρ, and length L

$I(z=0) = I_0$ $\quad G = \cosh^2\left\{\left(Ld\sqrt{2\omega_1(\omega_2-\omega_1)\eta^3}\sqrt{0.5cn\varepsilon_0E_{pump}^2}\right)\right\} \quad$ $I(z=L) = GI_0$

L
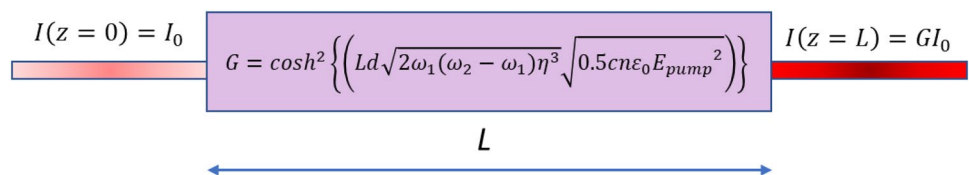
Table 1 OPA amplitude gain factor based on various wave/medium parameters

L	ρ (C/V^2)	ω_1 (THz)	ω_2 (THz)	ε	$E_{pump}\left(\frac{V}{m}\right)$	Gain$_{amplitude}$
1 mm	5×10^{-22}	600	800	13	3×10^8	8.76
3 mm	3×10^{-22}	600	800	13	3×10^8	86
5 mm	2×10^{-22}	600	800	13	3×10^8	153
1 cm	1×10^{-22}	400	600	10	5×10^8	813
3 cm	5×10^{-23}	400	600	10	5×10^8	7.47×10^5
5 cm	3×10^{-23}	400	600	10	4×10^8	4.35×10^4
7 cm	3×10^{-23}	400	600	10	3×10^8	7.68×10^4
10 cm	3×10^{-23}	400	600	13	3×10^8	6.1×10^5
20 cm	3×10^{-23}	300	500	13	3×10^8	5.3×10^6

2021; Annamalai and Vasilyev 2012; Schmidt et al. 2014; Li et al. 2011). Assuming that the spectral features of an interaction medium are fully known, it will be shown that the pump wave frequency can be adjusted to attain a resonant nonlinear response for an efficient parametric amplification of an input wave in the nanoscale. Here the OPA process is modeled by linking the wave equation to Lorentz dispersion equations via the electric polarization density term. To generalize, given that an interaction medium has M resonances (an arbitrary multiresonant media), by using M equations to model the electric polarization via Lorentz dispersion equations, and using the electric field wave equation to model the wave propagation, overall, the OPA process can be modeled using M + 1 equations (Saleh and Teich 2019; Aşırım and Yolalmaz 2020; Asırım and Kuzuoglu 2020; Asırım and Kuzuoglu 2020; Boyd 2008). To analyze the amplification of an input wave, firstly, the propagation of the total (input + pump) wave is considered (Fig. 2a) via Eqs. (3)–(5). Then the case of sole pump wave propagation is considered (Fig. 2b) using Eqs. (3, 6, 7). The mathematical model for the input wave propagation is constructed via subtracting Eqs. (6) and (7) from Eqs. (4) and (5) and by forming the equivalent problem (Eqs. 3, 8–11) for the input wave propagation under the influence of a high-amplitude pump wave.

Assuming an interaction medium with M resonances $\omega = \{\omega_1, \omega_2, \ldots, \omega_M\}$, associated with M polarization damping rates $\gamma = \{\gamma_1, \gamma_2, \ldots, \gamma_M\}$, the ensemble polarization density for the input and pump waves can be expressed as

$$P_{in} = \sum_{m=1}^{M} P_{in,m}, \quad P_p = \sum_{m=1}^{M} P_{p,m}. \tag{3}$$

Hence, the set of equations that model the total wave, pump wave, and the input wave can be written as follows.

Total wave propagation:

$$\nabla^2 \left(E_{in} + E_p\right) - \mu_0 \varepsilon_\infty \frac{\partial^2 \left(E_{in} + E_p\right)}{\partial t^2}$$
$$= \mu_0 \sigma \frac{\partial \left(E_{in} + E_p\right)}{\partial t} + \mu_0 \frac{d^2 \left(P_{in} + P_p\right)}{dt^2} \tag{4}$$

$$\frac{d^2 \left(P_{in,m} + P_{p,m}\right)}{dt^2} + \gamma_m \frac{d \left(P_{in,m} + P_{p,m}\right)}{dt} + \omega_m^2 \left(P_{in,m} + P_{p,m}\right)$$
$$- \frac{\omega_m^2 \left(P_{in,m} + P_{p,m}\right)^2}{N_m e d} + \frac{\omega_m^2 \left(P_{in,m} + P_{p,m}\right)^3}{N_m^2 e^2 d^2} = \frac{N_m e^2 \left(E_{in} + E_p\right)}{m_e}. \tag{5}$$

Pump wave propagation (input wave is removed):

$$\nabla^2 \left(E_p\right) - \mu_0 \varepsilon_\infty \frac{\partial^2 \left(E_p\right)}{\partial t^2} = \mu_0 \sigma \frac{\partial \left(E_p\right)}{\partial t} + \mu_0 \frac{d^2 P_p}{dt^2} \tag{6}$$

$$\frac{d^2 P_{p,m}}{dt^2} + \gamma_m \frac{dP_{p,m}}{dt} + \omega_m^2 P_{p,m} - \frac{\omega_m^2 P_{p,m}^2}{N_m e d} + \frac{\omega_m^2 P_{p,m}^3}{N_m^2 e^2 d^2} = \frac{N_m e^2 E_p}{m_e} \tag{7}$$

Equivalent problem for input wave propagation (under the influence of the pump wave):

$$\nabla^2 \left(E_{in}\right) - \mu_0 \varepsilon_\infty \frac{\partial^2 \left(E_{in}\right)}{\partial t^2} = \mu_0 \sigma \frac{\partial \left(E_{in}\right)}{\partial t} + \mu_0 \frac{d^2 P_{in}}{dt^2} \tag{8}$$

$$\frac{d^2 P_{in,1}}{dt^2} + \gamma_1 \frac{dP_{in,1}}{dt} + \omega_1^2 P_{in,1} - \frac{\omega_1^2 (2P_{in,1} P_{p,1} + P_{in,1}^2)}{N_1 e d}$$
$$+ \frac{\omega_1^2 (3P_{in,1} P_{p,1}^2 + 3P_{in,1}^2 P_{p,1} + P_{in,1}^3)}{N_1^2 e^2 d^2} = \frac{N_1 e^2 E_{in}}{m_e} \tag{9}$$

$$\frac{d^2 P_{in,2}}{dt^2} + \gamma_2 \frac{dP_{in,2}}{dt} + \omega_2^2 P_{in,2} - \frac{\omega_2^2 (2P_{in,2} P_{p,2} + P_{in,2}^2)}{N_2 e d}$$
$$+ \frac{\omega_2^2 (3P_{in,2} P_{p,2}^2 + 3P_{in,2}^2 P_{p,2} + P_{in,2}^3)}{N_2^2 e^2 d^2} = \frac{N_2 e^2 E_{in}}{m_e} \tag{10}$$

$$\frac{d^2 P_{in,M}}{dt^2} + \gamma_M \frac{dP_{in,M}}{dt} + \omega_M^2 P_{in,M} - \frac{\omega_M^2 (2P_{in,M} P_{p,M} + P_{in,M}^2)}{N_M e d}$$
$$+ \frac{\omega_M^2 (3P_{in,M} P_{p,M}^2 + 3P_{in,M}^2 P_{p,M} + P_{in,M}^3)}{N_M^2 e^2 d^2} = \frac{N_M e^2 E_{in}}{m_e} \tag{11}$$

(a)

(b)

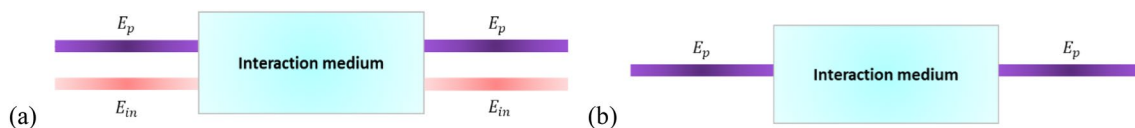**Fig. 2 a** Total optical wave excitation, $E = E_{in} + E_p$. **b** Pump wave excitation, $E = E_p$. E_{in} : Input wave electric field, E_p : Pump wave electric field, μ_0 : Free space permeability, ε_∞ : Background permittivity, t : time, σ : Conductivity, P_{in} : Input wave polarization density,

P_p : Pump wave polarization density, γ : Polarization damping rate, ω : Angular resonance frequency, N : Electron density, e : Elementary charge, d : Atom diameter, m_e : Electron mass

$$N = \sum_{m=1}^{M} N_m = \sum_{m=1}^{M} N\xi_m, \quad \sum_{m=1}^{M} \xi_m = 1 \qquad (12)$$

ξ_m : Oscillation strength for the mth resonance

As one can see from Eqs. (4)–(11), the pump wave is coupled to the input wave through the polarization density term. When the pump wave amplitude is very high (as dictated by OPA), the fourth and the fifth terms in Eqs. (9)–(11) cannot be ignored, requiring the nonlinear coupling effect to be taken into account.

Finite difference time domain discretization

As the input wave and the pump wave are propagating simultaneously through the interaction medium, due to the nonlinear coupling of the two waves (induced by the high amplitude of the pump wave), in order to solve for the time variation of the input wave, a concurrent solution of the pump wave is necessary. Therefore, Eqs. (6)–(11) must be solved in conjunction. To evaluate the input wave through Eqs. (8)–(11) at a given instant, prior knowledge of the pump wave is required. Hence, one must first solve for Eqs. (6)–(7) to evaluate the pump wave at the given instant. Using the finite difference time domain discretization, and assuming a one-dimensional spatial solution domain along the z direction, Eqs. (6)–(7) can be discretized in time and space as follows

$$
\begin{aligned}
&\frac{P_{\text{in},m}(i,j+1) - 2P_{\text{in},m}(i,j) + P_{\text{in},m}(i,j-1)}{\Delta t^2} \\
&+ \gamma_m \frac{P_{\text{in},m}(i,j) - P_{\text{in},m}(i,j-1)}{\Delta t} + 4\pi^2 f_m^2 \left(P_{\text{in},m}(i,j)\right) \\
&- \frac{4\pi^2 f_m^2}{N_m ed} \left\{ \left(P_{\text{in},m}(i,j)\right)^2 + 2P_{\text{in},m}(i,j)P_{\text{p},m}(i,j) \right\} \\
&+ \frac{4\pi^2 f_m^2}{N_m^2 e^2 d^2} \{ \left(P_{\text{in},m}(i,j)\right)^3 \\
&+ 3\left(P_{\text{in},m}(i,j)\right)^2 P_{\text{p},m}(i,j) + 3P_{\text{in},m}(i,j)\left(P_{\text{p},m}(i,j)\right)^2 \} \\
&= \frac{N_m e^2}{m_e}\left(E_{\text{in}}(i,j)\right).
\end{aligned}
\qquad (17)
$$

$$P_{\text{in}} = P_{\text{in},1} + P_{\text{in},2} + \cdots + P_{\text{in},M}, \quad N = N_1 + N_2 + \cdots + N_M. \qquad (18)$$

z: space coordinate, t: time, m: resonance number, $P_m(z,t) = P_m(i\Delta z, j\Delta t) \rightarrow P_m(i,j)$.

The FDTD discretization should be carried in accordance with the numerical stability restrictions. Based on the wavelengths of the input and the pump waves, the selected spatial discretization must be small enough to capture the wave propagation in high resolution and to ensure that the solution does not blow up (Li et al. 2011; Zygiridis and Kantartzis 2018). As the problem is nonlinear, the numerical stability criterion, which is mainly derived for solving linear wave propagation problems, cannot be taken for granted as a valid stability measure. For nonlinear wave propagation problems, a good strategy is to select the spatial discretization to be much smaller than the upper limit that is suggested by the

$$
\begin{aligned}
&\frac{E_{\text{p}}(i+1,j) - 2E_{\text{p}}(i,j) + E_{\text{p}}(i-1,j)}{\Delta z^2} - \mu_0 \epsilon_\infty(i,j)\frac{E_{\text{p}}(i,j+1) - 2E_{\text{p}}(i,j) + E_{\text{p}}(i,j-1)}{\Delta t^2} \\
&= \mu_0 \sigma(i,j)\frac{E_{\text{p}}(i,j) - E_{\text{p}}(i,j-1)}{\Delta t} + \mu_0 \frac{P_{\text{p}}(i,j+1) - 2P_{\text{p}}(i,j) + P_{\text{p}}(i,j-1)}{\Delta t^2}
\end{aligned}
\qquad (13)
$$

$$
\begin{aligned}
&\frac{P_{\text{p},m}(i,j+1) - 2P_{\text{p},m}(i,j) + P_{\text{p},m}(i,j-1)}{\Delta t^2} + \gamma_m \frac{P_{\text{p},m}(i,j) - P_{\text{p},m}(i,j-1)}{\Delta t} + 4\pi^2 f_m^2 \left(P_{\text{p},m}(i,j)\right) \\
&- \frac{4\pi^2 f_m^2}{N_m ed}\left(P_{\text{p},m}(i,j)\right)^2 + \frac{4\pi^2 f_m^2}{N_m^2 e^2 d^2}\left(P_{\text{p},m}(i,j)\right)^3 = \frac{N_m e^2}{m_e}\left(E_{\text{p}}(i,j)\right).
\end{aligned}
\qquad (14)
$$

$$P_p = P_{p,1} + P_{p,2} + \cdots + P_{p,M}, \quad N = N_1 + N_2 + \cdots + N_M. \qquad (15)$$

Followingly, Eqs. (8)–(11) are discretized to solve for the input wave

numerical stability criterion and to double-check the stability of the solution throughout the simulation time. This may not be an ideal approach concerning the required computer memory and the associated computation time. However, it is

$$
\begin{aligned}
&\frac{E_{\text{in}}(i+1,j) - 2E_{\text{in}}(i,j) + E_{\text{in}}(i-1,j)}{\Delta z^2} - \mu_0 \epsilon_\infty(i,j)\frac{E_{\text{in}}(i,j+1) - 2E_{\text{in}}(i,j) + E_{\text{in}}(i,j-1)}{\Delta t^2} \\
&= \mu_0 \sigma(i,j)\frac{E_{\text{in}}(i,j) - E_{\text{in}}(i,j-1)}{\Delta t} + \mu_0 \frac{P_{\text{in}}(i,j+1) - 2P_{\text{in}}(i,j) + P_{\text{in}}(i,j-1)}{\Delta t^2}
\end{aligned}
\qquad (16)
$$

a safe one that not only ensures accuracy and precision, but also brings out a high-resolution wave simulation. Naturally, this strategy can be relaxed depending on the requirements and restrictions of the investigated problem.

Accuracy of the computational model and comparison with experimental results

The semiempirical formula for OPA in Eq. (1) is not valid in the micro and nanoscale. Therefore, our numerical model is tested using the experimental formula for the sum frequency generation via nonlinear wave mixing process, which is the process that gives to OPA and has the same underlying physical mechanism (Saleh and Teich 2019; Boyd 2008). In this subsection, the origination of a monochromatic wave with frequency (ω_3) is investigated via mixing of two other monochromatic waves with frequencies ω_1 and ω_2 under nonlinear coupling, such that $\omega_3 = \omega_2 + \omega_1$. As before, the high-amplitude wave is called the pump wave (ω_2) and the relatively low-amplitude wave is called the input wave (ω_1). The pump wave E_2 is originated at $x = 2.5\ \mu m$, with an amplitude of A_2 V/m and a frequency of 450 THz.

$$E_2(x = 2.5\ \mu m, t) = A_2 \times \sin\left(2\pi\left(4.5 \times 10^{14}\right)t + \varphi_2\right) \text{V/m (Pump wave)}$$

The input wave E_1 is also generated at $x = 2.5\ \mu m$, with an amplitude of A_1 V/m and a frequency of 200 THz.

$$E_1(x = 2.5\mu m, t) = A_1 \times \sin\left(2\pi\left(2 \times 10^{14}\right)t + \varphi_1\right) \text{V/m} \quad \text{(Input wave, assume } \varphi_1 = \varphi_2 = 0)$$

Spatial and temporal range of the computation: $0 \le x \le 10\ \mu m, 0 \le t \le 5$ ps

Transition/Resonance frequency of the interaction medium : $f_0 = 3.45 \times 10^{14} \text{Hz (Gallium Arsenide)}$

Polarization damping rate of the interaction medium : $\gamma = 1 \times 10^9 \text{Hz}$

Background dielectric coefficient of the interaction medium $(\varepsilon_\infty) = 1 + \chi = 13 \quad (\mu_r = 1)$

To prevent reflections and to limit the size of the computational domain, an absorbing layer, known as the perfectly matched layer (PML) (Zygiridis and Kantartzis 2018) is used on each side of the interaction medium. Details on PML can be found in Zygiridis and Kantartzis (2018) (Fig. 3).

Left PML(left absorption layer)is from $x = 0$ to $x = 2.25\ \mu m$

Right PML(right absorption layer)is from $x = 7.75\ \mu m$ to $x = 10\ \mu m$
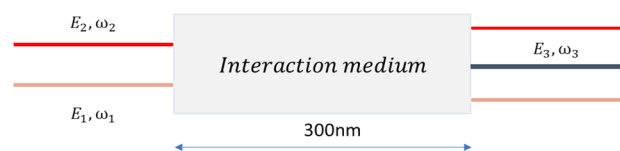

Fig. 3 Configuration for optical sum frequency generation

The empirical mathematical expression for sum frequency generation efficiency is stated as (Saleh and Teich 2019; Boyd 2008)

$$\begin{aligned} \eta_{\text{experimental}} &= \frac{\omega_3}{\omega_2}\left(\sin\sqrt{2\rho^2 n^3 \omega_3^2 \left(cn\varepsilon_0 A_2^2\right)L^2}\right)^2 \\ &= \frac{\omega_3}{\omega_2}\left(\sin\sqrt{2\rho^2 n^4 \omega_3^2 c\varepsilon_0 A_2^2 L^2}\right)^2 \end{aligned} \tag{19}$$

ρ = nonlinearity of the interaction medium, n = refractive index of the interaction medium.

A_2 = pump wave amplitude, A_1 = input wave amplitude, L = length of the interaction medium.

The computational sum frequency generation (frequency up-conversion) efficiency is formulated as (Aşırım and Yolalmaz 2020; Aşırım and Kuzuoglu 2020; Aşırım and Kuzuoglu 2020)

$$\eta_{\text{computational}} = \frac{\text{Intensity of the total wave around } \omega = \omega_3 \text{ at } t = t_{\max}}{\text{Intensity of the total wave around } \omega = \omega_2 \text{ at } t = 0}. \tag{20}$$

Here, the following values are used in the computation of each efficiency using Eqs. (13–18, 19):

$\omega_2 = (2\pi \times 450)$ THz, $\omega_1 = (2\pi \times 200)$ THz,

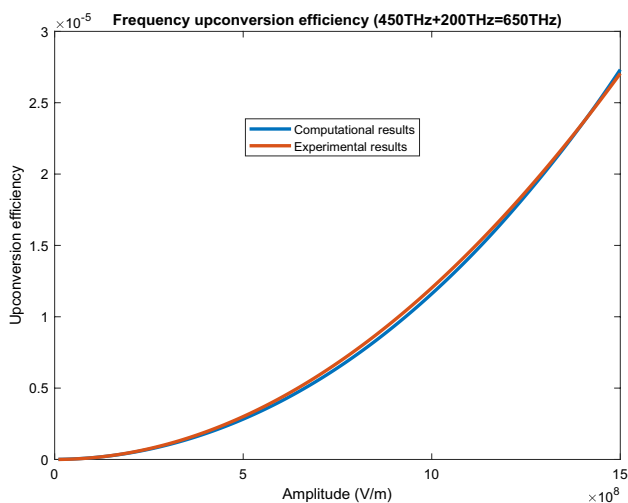$L = 300$ nm (from $x = 5\ \mu m$ to $5.3\ \mu m$)

Fig. 4 Comparison of the computational and experimental frequency up-conversion efficiencies for $f_3 = 650\,\text{THz}$ and $\rho = 1.79 \times 10^{-22}\,\text{C/V}^2$, against the pump wave amplitude

$\omega_3 = $ Frequency of the up - converted harmonic $= (2\pi \times 650)\text{THz}$, $n = \sqrt{13}$, $\rho = 1.79 \times 10^{-22}\,\text{C/V}^2$. (This value is chosen such that the computational and the experimental results match for a sample pump wave amplitude of $A_2 = 10^8\,\text{V/m}$. To verify the accuracy of the computational model, the results must also agree for all the other pump wave amplitudes, for this same value of ρ) (Fig. 4).

$A_2 = $ Pump wave amplitude (swept from $1 \times 10^7\,\text{V/m}\, to\, 1.5 \times 10^9\,\text{V/m}$), $A_1 = $ Input wave amplitude $= A_2/5$.

Results

OPA in an interaction medium with multiple resonance frequencies

In this section, the feasibility of high-gain OPA is examined in the nanoscale using Eqs. (13)–(18) for an arbitrary interaction medium. Here, we assume that the low-amplitude input wave E_{in} and the high-amplitude pump wave E_{p} are concurrently propagating through the 300 nm long interaction medium with three resonance frequencies (transitions). The waves are originated at $x = 3\,\mu\text{m}$ at time $t = 0$ s. The monochromatic input wave E_{in} to be amplified, has an electric field amplitude of 1 V/m and a frequency of 440 THz. The high-amplitude pump wave E_{p} has an amplitude of 2×10^8 V/m, and its frequency ν_{p} is to be selected after a sweep analysis, based on the optimal value that simultaneously maximizes the electric energy density and the polarization density induced by the pump wave. The features of both waves, and the values of the interaction medium parameters are as provided below:
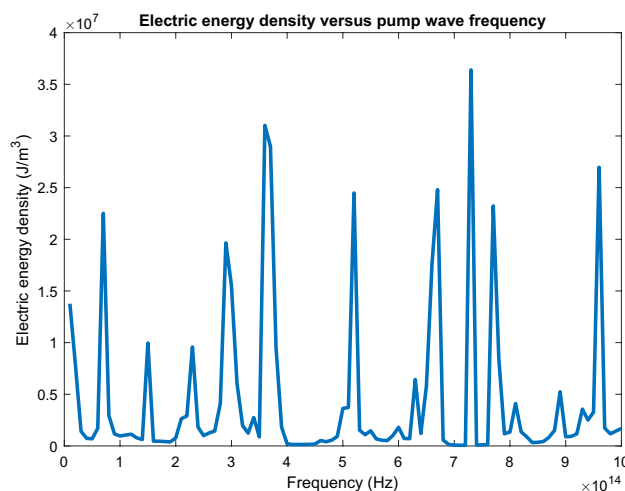

Fig. 5 Pump wave-induced electric energy density versus pump wave frequency

$$E_{\text{in}}(x = 3\,\mu\text{m}, t) = 1 \times \sin\left(2\pi\left(4.4 \times 10^{14}\right)t\right)\text{V/m}$$

$$E_{\text{p}}(x = 3\,\mu\text{m}, t) = 2 \times 10^8 \times \sin\left(2\pi\left(\nu_{\text{p}}\right)t\right)\text{V/m}$$

Spatial and temporal discretization range：
$0 \leq x \leq 10\,\mu\text{m},\, 0 \leq t \leq 5\,\text{ps}$

Interaction medium resonances：
$f_{\text{r}} = \left\{4 \times 10^{14}\text{Hz}, 7 \times 10^{14}\text{Hz}, 1.2 \times 10^{15}\text{Hz}\right\}$

Polarization damping rates for each resonance：
$\gamma = \left\{1 \times 10^9\text{Hz}, 4 \times 10^9\text{Hz}, 1.2 \times 10^{10}\text{Hz}\right\}$

Relative permittivity：$\left(\varepsilon_{\text{r}}\right) = 13(\mu_{\text{r}} = 1)$,
Atom diameter：$d = 0.3$ nanometers

Interaction medium range ： $5\mu\text{m} < x < 5.3\mu\text{m}$ ，
Number of electrons per volume ： $N = 3.5 \times 10^{28}/\text{m}^3$.

The goal is to identify all the pump wave excitation frequencies within the IR-VISIBLE band that simultaneously yield the highest electric energy density and the highest polarization density within the interaction medium.

Based on the solution of Eqs. (6)–(12), the electric energy density induced by the pump wave is computed as

$$W_{e,p} = \frac{1}{2}\varepsilon_\infty E_p^2 + \frac{1}{2}E_p P_p. \tag{21}$$

Figure 5 shows the plot of the electric energy density against the pump wave frequency. Concerning the practical
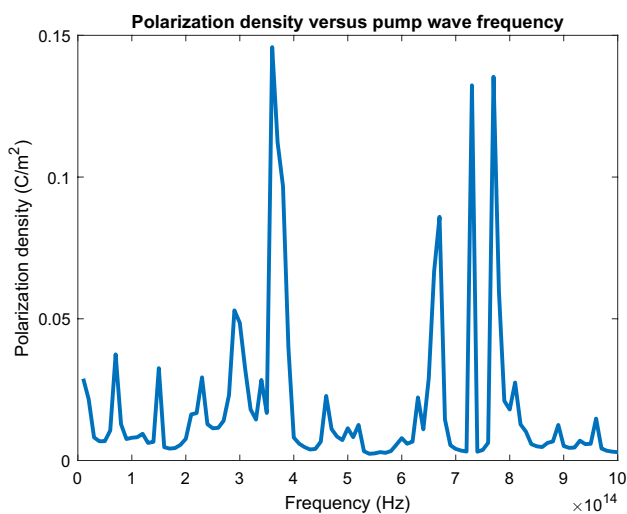
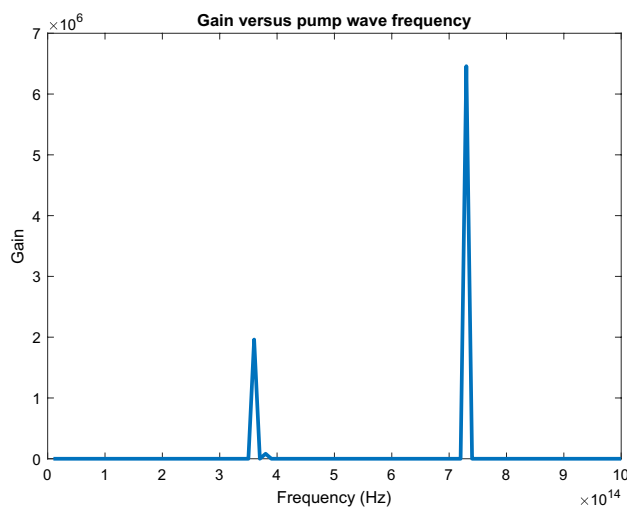**Fig. 6** Pump wave induced polarization density versus pump wave frequency
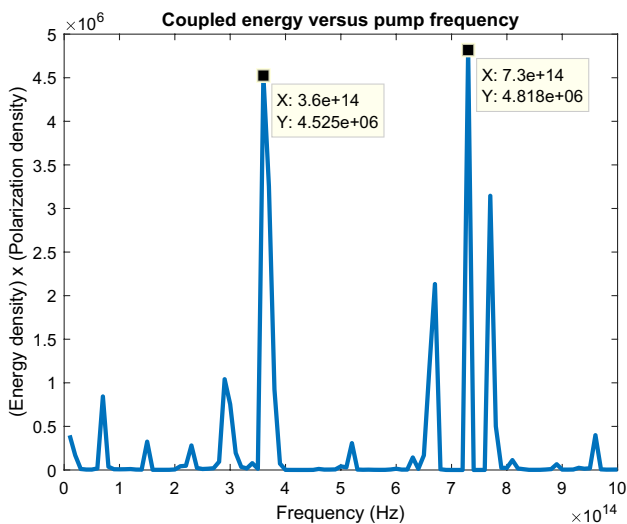

Fig. 8 Gain versus pump wave frequency

Fig. 7 Plot of the multiplication of the energy density with the polarization density, versus pump wave frequency

Table 2 Input wave gain factor versus pump wave frequency, energy density, and polarization density

f_p (THz)	Gain	$W_{e,p}\left(\frac{J}{m^3}\right)$	$P_p\left(\frac{C}{m^2}\right)$
100	1.78	9.66×10^5	0.0080
150	1.80	9.96×10^6	0.0326
200	1.77	7.75×10^5	0.0076
250	1.78	4.48×10^7	0.0114
300	1.79	1.7×10^7	0.0485
350	1.78	8.54×10^5	0.0167
360	1.96×10^6	3.10×10^7	0.1458
400	1.78	1.81×10^5	0.0081
500	1.79	3.63×10^6	0.0114
600	1.79	1.80×10^6	0.0079
700	1.78	8.42×10^4	0.0041
730	6.52×10^6	3.64×10^7	0.1324
770	6.83×10^3	2.32×10^7	0.1354
800	1.77	1.35×10^6	0.018
900	1.78	8.93×10^5	0.0051
1000	1.78	1.69×10^6	0.0029

spectral range, the pump wave frequency is swept until 1000 THz. Within the investigated spectral range, the highest energy densities occur around 360 THz and 730 THz. The energy density is minimum around the resonance frequencies (400 THz, 700 THz) of the medium. All output parameters are computed at $x = 5.5$ μm.

The polarization density (P_p) is computed via Eqs. (6)–(7) and plotted in Fig. 6. The highest polarization densities occur around 360 THz, 730 THz, and 770 THz, whereas the lowest ones occur around 400 THz and 700 THz.

To find the pump wave frequencies which yield the highest energy transfer to the input wave, we multiply the polarization density (P_p, which acts as the nonlinear coupling

strength) with the electric energy density $W_{e,p}$. The result is plotted in Fig. 7. The highest energy coupling to the input wave occurs around 360 THz and 730 THz.

Since the input wave amplitude was normalized as 1 V/m at $t = 0$ s, the amplitude of the input wave at $t = 5$ ps is taken as the gain factor. Figure 5 shows the resulting gain factor ($E_{in}(x = 5.5$ μm, $t = 5$ ps)) versus the pump wave amplitude, computed via Eqs. (6)–(12). The gain factor is significantly high only at those frequencies where the multiplication of the electric energy density and the polarization density (energy coupling strength) is relatively high (Fig. 8).

Table [2] provides a comparison of each parameter in more detail. It is evident that the simultaneous maximization of energy density and polarization density, induces an efficient nonlinear energy-coupling that enables a high gain factor. Based on Table [2], for the given interaction medium parameters, the required energy density for high-gain OPA is above 30 MJ/m^3, and the required polarization density is higher than 0.13 C/m^2.

OPA using GaAs nanofilm

In the previous subsection, nanoscale OPA was investigated for an arbitrary multi-resonant medium. Here, the phenomenon is investigated for Gallium Arsenide. Once again, the input wave E_{in} and the pump wave E_p are simultaneously generated at $x = 3$ μm at time $t = 0$ s. The length of the interaction medium (GaAs) is 300 nm. The initial (excitation) amplitude of the input wave electric field is set as 1 V/m, with a frequency of 200 THz. The pump wave excitation amplitude is set as 4.5×10^8 V/m (frequency to be selected). The parameters of the interaction medium and the waves are as given below

$$E_{in}(x = 3\mu m, t) = 1 \times \sin\left(2\pi\left(2 \times 10^{14}\right)t\right) V/m$$

$$E_p(x = 3\mu m, t) = 4.5 \times 10^8 \times \sin\left(2\pi\left(v_p\right)t\right) V/m$$

Spatial and temporal discretization range :
$0 \leq x \leq 10\mu m, 0 \leq t \leq 5ps$

Interaction medium resonance frequency : $f_r = 3.45 \times 10^{14}$ Hz

Polarization damping rate of the interaction medium :

$\gamma = 1 \times 10^{10}$ Hz

Relative permittivity : $\left(\varepsilon_r\right) = 13(\mu_r = 1)$,
Atomic diameter : $d = 0.3$ nanometers

Interaction medium range : $5\mu m < x < 5.3\mu m$,
Electron density : $N = 3.5 \times 10^{28}/m^3$.

Since there is only a single resonance at 345 THz for GaAs, the equations that model the spatio-temporal variation of the input and pump waves can be written as

$$\nabla^2\left(E_p\right) - \mu_0\varepsilon_\infty\frac{\partial^2\left(E_p\right)}{\partial t^2} = \mu_0\sigma\frac{\partial\left(E_p\right)}{\partial t} + \mu_0\frac{d^2P_p}{\partial t^2} \quad (22)$$

$$\frac{d^2P_p}{dt^2} + \gamma\frac{dP_p}{dt} + \omega_r^2 P_p - \frac{\omega_r^2 P_p^2}{Ned} + \frac{\omega_r^2 P_p^3}{N^2 e^2 d^2} = \frac{Ne^2 E_p}{m} \quad (23)$$

$$\nabla^2\left(E_{in}\right) - \mu_0\varepsilon_\infty\frac{\partial^2\left(E_{in}\right)}{\partial t^2} = \mu_0\sigma\frac{\partial\left(E_{in}\right)}{\partial t} + \mu_0\frac{d^2P_{in}}{dt^2} \quad (24)$$

$$\frac{d^2P_{in}}{dt^2} + \gamma\frac{dP_{in}}{dt} + \omega_r^2 P_{in} - \frac{\omega_r^2(2P_{in}P_p + P_{in}^2)}{Ned}$$
$$+ \frac{\omega_r^2(3P_{in}P_p^2 + 3P_{in}^2 P_p + P_{in}^3)}{N^2 e^2 d^2} = \frac{Ne^2 E_{in}}{m}. \quad (25)$$

Once again, the pump wave induced electric energy density is evaluated as

$$W_{e,p} = \frac{1}{2}\varepsilon_\infty E_p^2 + \frac{1}{2}E_p P_p.$$

Figure [9] shows the plot of the electric energy density against the pump wave frequency. In the case of GaAs, the highest energy densities occur for the pump wave frequencies $v_p = 300$ THz and $v_p = 630$ THz. The energy density is relatively very low for the interval 320 THz < v_p < 580 THz, which includes the resonance frequency of GaAs. All output parameters are computed at $x = 5.5\ \mu m$.

The polarization density (P_p) is plotted in Fig. [10]. The highest polarization density occurs at the pump wave frequency $v_p = 520$ THz. Based on the multiplication of the electric energy density and the polarization density (Fig. [11]), which is the measure of energy transfer to the input wave, the highest energy transfer to the input wave occurs for the pump wave frequencies $v_p = 300$ THz and $v_p = 630$ THz. As the input wave amplitude was normalized as 1 V/m at $t = 0$ s, the input wave amplitude at $t = 5$ ps is accepted as the gain factor. Figure [12] illustrates
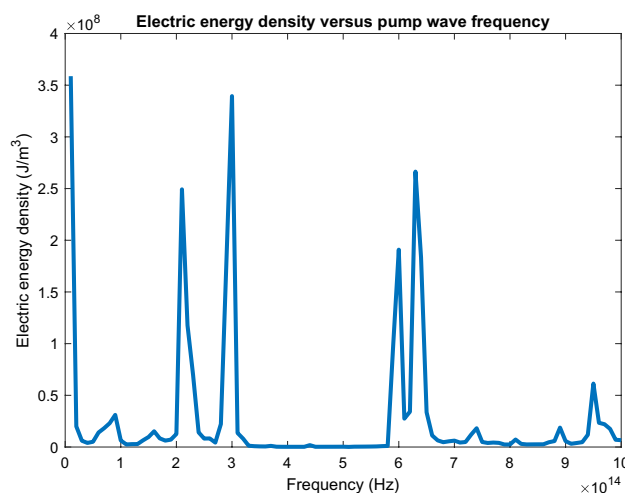

Fig. 9 Electric energy density versus pump wave frequency. The electric energy density within the interaction medium (GaAs) is maximized for pump wave frequencies $v_p = 300$ THz, and $v_p = 630$ THz
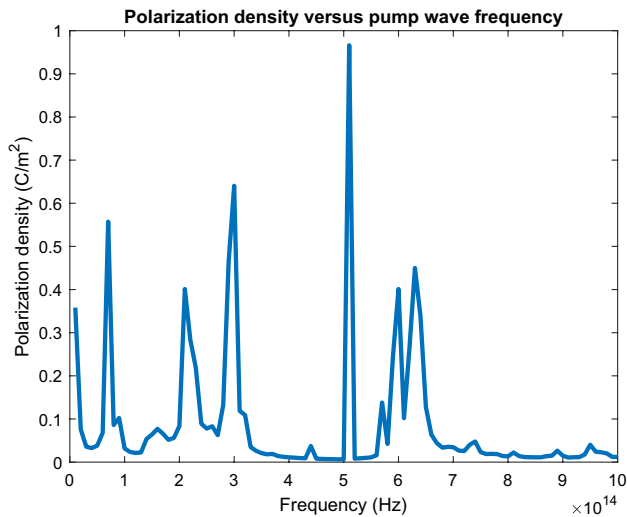
Polarization density versus pump wave frequency

Fig. 10 Polarization density versus pump wave frequency. The polarization density is maximized for the pump wave frequencies $v_p = 300$ THz and $v_p = 520$ THz, enabling an efficient nonlinear coupling of electric energy at these frequencies
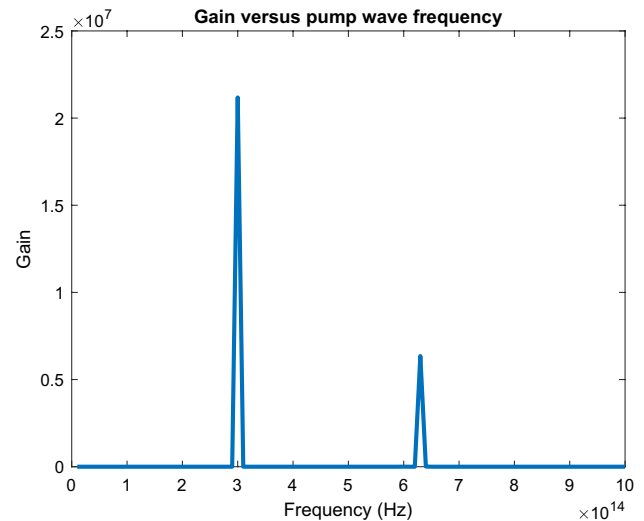
Coupled energy versus pump frequency

X: 3e+14
Y: 2.174e+08

X: 6.3e+14
Y: 1.199e+08

Fig. 11 Plot of the multiplication of the energy density with the polarization density, versus pump wave frequency. The figure illustrates the pump wave frequencies at which the amount of electric energy that is coupled to the input wave is maximized, enabling a super-nonlinear interaction medium response for the input wave

the input wave amplitude ($E_{in}(x = 5.5\ \mu m, t = 5$ ps)) against the pump wave amplitude, computed via Eqs. (6)–(12). The input wave amplitude is maximized at the pump wave frequencies where the multiplication of the electric energy density and the polarization density is relatively high. Notice that the input wave amplitude

Gain versus pump wave frequency

Fig. 12 Gain versus pump wave frequency. Significant OPA gain occurs at the pump wave frequencies $v_p = 300$THz and $v_p = 630$THz, where coupling of electric energy to the input wave is the highest

Table 3 Input wave amplitude gain, versus pump wave frequency, energy density, and polarization density

f_p (THz)	Gain	$W_{e,p}\left(J/m^3\right)$	$P_{pump}\left(C/m^2\right)$
100	0.0260	6,324,972	0.0315
200	0.0140	12,615,479	0.0835
300	21,182,400	3.39×10^8	0.6404
400	0.0140	203,469	0.0111
500	0.0141	294,853	0.0067
600	4409	1.91×10^8	0.4011
630	6,348,300	2.66×10^8	0.4500
700	0.0141	6,171,942	0.0345
800	0.0141	2,427,828	0.0133
900	0.0141	5,652,442	0.0147
1000	0.0141	6,609,689	0.0117

is otherwise quite weak, which implies that a significant OPA does not occur for other pump wave frequencies (Table 3).

Discussion

The simultaneous maximization of the energy density and the polarization density within an interaction medium provides a super-nonlinear electrical response for the input wave, which causes it to amplify at super-short distances. The required energy density for nanoscale OPA seems to be on the order of MJ/m³. But even at such high energy densities, if the polarization density is not synchronously maximized, high-gain OPA seems to be unattainable. This

Fig. 13 High-gain parametric amplification of an input beam through the simultaneous maximization of pump-induced intracavity electric energy density, and the polarization density
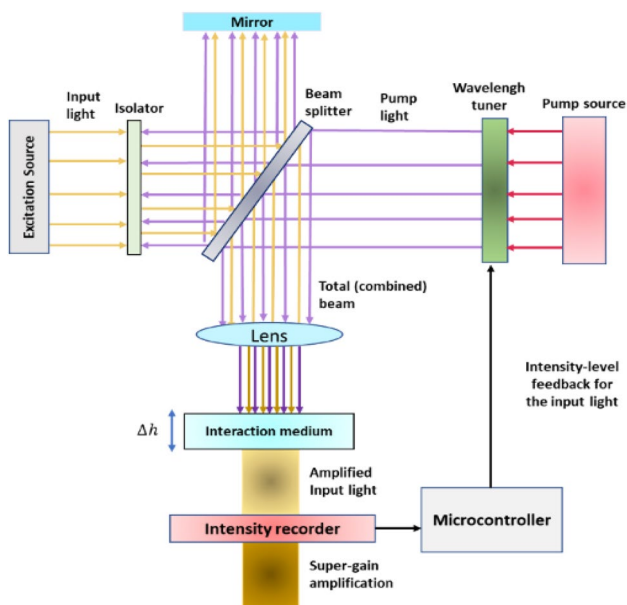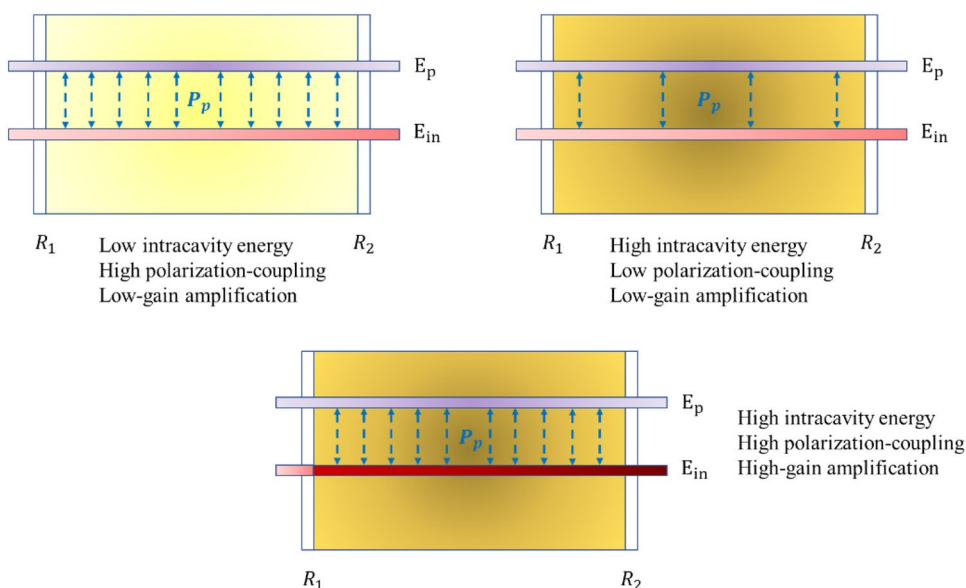

Fig. 14 Practical implementation of adaptive OPA through tuning of the pump wave frequency for gain enhancement

also behaves like a cavity due to its relative permittivity and its ultra-short interaction length in an unbounded space.

Therefore, choosing the correct pump wave frequency that enables nanoscale high-gain OPA, is the same as choosing the pump wave frequency that maximizes the product of the energy density and the polarization density, which was demonstrated by both of the outlined investigations. The pump wave induced polarization density P_p acts as the energy coupling parameter, since it couples to the input wave polarization density, as mathematically stated by the equivalent problem in Eqs. (8)–(12). The pump wave polarization density is naturally correlated with the amplitude of the pump wave. When the pump wave amplitude is not sufficiently high, its associated polarization density is quickly extinguished within an interaction medium, which suggests that the interaction medium response is quasi-linear, and the coupling of the input and the pump wave is weak. However, even under high-amplitude pump wave excitations, a relatively low polarization density is usually present due to dielectric absorption (particularly around the resonance frequencies of the interaction medium), and the associated phase mismatch between the input wave and the pump wave in relation to the electrical response of the nanoscale interaction medium. Although the ultra-small interaction medium length enables phase matching over a very large bandwidth, minimizing the phase mismatch by selecting the optimal pump wave frequency that maximizes the polarization coupling as modeled by the Lorentz equation, is generally noteworthy, which is automatically handled by a precise determination of the optimal pump wave frequency under the presented numerical model. Hence, a careful dispersion analysis is essential for nanoscale high-gain OPA via a

is because without enhanced pump-induced polarization density P_p, the induced high energy density cannot be coupled to the input wave for amplification, as the coupling of energy occurs through the cross-polarization terms in Eqs. (9)–(11), which are absent in a linear problem. Hence, the pump-induced polarization density P_p represents the coupling strength and should be maximized for efficient energy coupling. Figure 13 illustrates the requirement of simultaneous maximization of both densities through the cavity analogy, as a nanoscale interaction medium for OPA

precise tuning of the pump wave frequency that maximizes the energy density, minimizes the phase mismatch, and enhances the pump wave-induced polarization density for efficient energy coupling.

Since the threshold energy density for high-gain OPA seems to be on the order of MJ/m^3, damage to the interaction medium is unlikely, as optical damage is usually present for energy densities on the order of GJ/m^3 (Dao et al. 2015; Choi et al. 2021). Interaction materials of high dielectric strength can be employed concerning optical damage. The biggest advantage of the presented method is that it does not require a specific material for high-gain OPA. The only requirement is the knowledge of the dispersion features of the interaction medium.

The fabrication of such a short-length interaction medium is feasible via physical vapor deposition (PVD) process, which can form an ultra-thin, uniform wafer on a substrate, through a sputtering gas and a sputtering target situated in a vacuum chamber (Ilangovan et al. 2021). The proposed setup for the practical implementation of the aforementioned OPA process is shown in Fig. 14. The necessary tuning of the pump frequency can be carried out via the interaction of an intensity recorder (which measures the intensity at the frequency of the input wave), a controller device, and a wavelength tuner. This way, the pump frequency can be continuously adjusted until the input wave amplitude is maximized.

Conclusion

Although OPA has always been noted for interaction mediums that are at least a few milimeters long, in this study, it is observed that nanoscale high-gain OPA occurs for pump wave frequencies that simultaneously maximize the electric energy density and the polarization density within the interaction medium. Both the condensation of the electric energy density and the maximization of the polarization density is attained by selecting the correct pump wave frequency through an in-depth dispersion analysis using the nonlinear Lorentz dispersion equations for each resonance frequency of the interaction medium, and a concurrent solution of the wave equations for both waves. This enables a super-nonlinear response by the interaction medium for a given input wave to be amplified. For an arbitrary interaction medium, to determine the pump wave frequencies that are likely to provide high-gain OPA, the product of the energy density and the polarization density should be computed for all pump wave frequencies, and the pump wave frequencies that yield the highest values of the product should be marked. The OPA performance for the input wave should then be assessed at these pump wave frequencies.

Declarations

Conflict of interest On behalf of all authors, the corresponding author states that there is no conflict of interest.

References

Annamalai M, Vasilyev M (2012) Phase-sensitive multimode parametric amplification in a parabolic-index waveguide. IEEE Photonics Technol Lett 24(21):1949–1952

Asırım OE, Kuzuoglu M (2020a) Enhancement of optical parametric amplification in micro-resonators via gain medium parameter selection and mean cavity wall reflectivity adjustment. J Phys B Atom Mol Opt Phys 53:185401

Asırım OE, Kuzuoglu M (2020) Super-gain optical parametric amplification in dielectric micro-resonators via BFGS algorithm-based non-linear programming. Appl Sci 10:1770

Aşırım OE, Yolalmaz A (2020) Design of ultra-high gain optical micro-amplifiers via smart non-linear wave mixing. Prog Electromagn Res B 89:177–194

Baumgartner R, Byer R (1979) Optical parametric amplification. IEEE J Quantum Electron 15(6):432–444

Boyd RW (2008) Nonlinear optics. Academic Press, New York, pp 11–96

Cheng YH, Gao FY, Poulin PR et al (2018) Efficient two-stage dual-beam noncollinear optical parametric amplifier. Appl Phys B 124:93

Choi JW, Sohn B-U, Sahin E, Chen GFR, Xing P, Ng DKT, Eggleton BJ, Tan DTH (2021) An optical parametric Bragg amplifier on a CMOS chip. Nanophotonics 10(13):3507–3518

Cholan NA, Mahdi MA, Al-Mansoori MH, Noor AS, Ismail A (2011) Fiber optical parametric amplifier with dispersion flattened photonics crystal fiber as a gain medium. In: 2nd international conference on photonics, IEEE. Kota Kinabalu, Malaysia, pp 1–3

Dao L, Dinh K, Hannaford P (2015) Perturbative optical parametric amplification in the extreme ultraviolet. Nat Commun 6:7175

De Ceglia D, Carletti L, Vincenti MA, De Angelis C, Scalora M (2019) Second-harmonic generation in Mie-resonant GaAs nanowires. Appl Sci 9:3381

Fragemann A, Pasiskevicius V, Karlsson G, Laurell F (2003) High-peak power nanosecond optical parametric amplifier with periodically poled KTP. Opt Express 11:1297–1302

Gonzalez M, Lee Y (2018) A study on parametric amplification in a piezoelectric MEMS device. Micromachines (basel) 10(1):19

Ilangovan R, Subha V, Earnest Ravindran RS, Kirubanandan S, Renganathan S (2021) Nanomaterials: synthesis, physicochemical characterization, and biopharmaceutical applications, micro and nano technologies, nanoscale processing, Chapter 2. Elsevier, New York, pp 33–70

Kuramochi E (2021) Photonic-crystal optical parametric oscillator. Nat Photonics 15:2–4

Li X, Long H, Liu H (2011) Numerical simulation of ultra-broadband phase-sensitive optical parametric amplification of image. J Russ Laser Res 32(6):547–555

Lin YC, Nabekawa Y, Midorikawa K (2020) Optical parametric amplification of sub-cycle shortwave infrared pulses. Nat Commun 11:3413

Manzoni C, Cerullo G (2016) Design criteria for ultrafast optical parametric amplifiers. J Opt 18:103501

Marhic ME, Andrekson PA, Petropoulos P, Radic S, Peucheret C, Jazayerifar M (2015) Fiber optical parametric amplifiers in optical communication systems. Laser Photonics Rev 9(1):50–74

Markov A, Mazhorova A, Breitenborn H, Bruhacs A, Clerici M, Modotto D, Jedrkiewicz O, di Trapani P, Major A, Vidal F, Morandotti R (2018) Broadband and efficient adiabatic three-wave-mixing in a temperature-controlled bulk crystal. Opt Express 26:4448–4458

Martinelli M et al (2001) Classical and quantum properties of optical parametric oscillators. Braz J Phys [online] 31(4):597–615

Milton MJT, McIlveen TJ, Hanna DC, Woods PT (1992) A high-gain optical parametric amplifier tunable between 3.27 and 3.65 μm. Opt Commun 93(3–4):186–190

Ooi K, Ng D, Wang T et al (2017) Pushing the limits of CMOS optical parametric amplifiers with USRN:Si7N3 above the two-photon absorption edge. Nat Commun 8:13878

Paschotta R (2008) Optical parametric amplifiers, encyclopedia of laser physics and technology, 1st edn. Wiley-VCH, New York

Ren M-L, Li Z-Y (2011) Analysis of three-wave mixing in one-dimensional nonlinear multilayer structures with pump depletion. J Appl Phys 109:083113

Rout A, Boltaev GS, Ganeev RA, Fu Y, Maurya SK, Kim VV, Rao KS, Guo C (2019) Nonlinear optical studies of gold nanoparticle films. Nanomaterials 9:291

Sakhno O, Yezhov P, Hryn V, Rudenko V, Smirnova T (2020) Optical and nonlinear properties of photonic polymer nanocomposites and holographic gratings modified with noble metal nanoparticles. Polymers 12:480

Saleh BEA, Teich MC (2019) Fundamentals of photonics, 3rd edn. Wiley, New York, pp 1056–1057

Schmidt B, Thiré N, Boivin M et al (2014) Frequency domain optical parametric amplification. Nat Commun 5:3643

Taghizadeh M, Hatami M, Pakarzadeh H, Tavassoly MKH (2017) Pulsed optical parametric amplification based on photonic crystal fibres. J Mod Opt 64(4):357–365

Trovatello C, Marini A, Xu X et al (2021) Optical parametric amplification by monolayer transition metal dichalcogenides. Nat Photonics 15:6–10

Valiulis G, Dubietis A, Piskarskas A (2008) Optical parametric amplification of chirped X pulses. Phys Rev A 77:043824

Varin C, Emms R, Bart G, Fennel T, Brabec T (2018) Explicit formulation of second and third order optical nonlinearity in the FDTD framework. Comput Phys Commun 222:70–83

Wang D, Zhang Y, Xiao M (2013) Quantum limits for cascaded optical parametric amplifiers. Phys Rev A 87:023834

Wang K, Tian Q, Zhang Qi, Zhang L, Xin X (2019) Optimized design of single-pump fiber optical parametric amplifier with highly nonlinear fiber segments using a differential evolution algorithm. Opt Eng 58(8):086104

Xiao Q, Pan X, Lu X, Cui Z, Fan W, Li X (2021) The study of frequency domain optical parametric amplification technology. In: Proceedings of SPIE 11849, Fourth International Symposium on High Power Laser Science and Engineering (HPLSE 2021), 118490D

Ye H, Kumar SC, Wei J, Schunemann PG, Ebrahim-Zadeh M (2018) 1 μm-pumped optical parametric generator and oscillator based on orientation-patterned gallium phosphide. In: Proceedings of SPIE 10684, nonlinear optics and its applications 2018, 106841W

Zhang JY, Huang JY, Shen YR, Chen C (1993) Optical parametric generation and amplification in barium borate and lithium triborate crystals. J Opt Soc Am B 10:1758–1764

Zhang Y et al (2016) Toward surface plasmon-enhanced optical parametric amplification (SPOPA) with engineered nanoparticles: a nanoscale tunable infrared source. Nano Lett 16(5):3373–3378

Zygiridis TT, Kantartzis NV (2018) Finite-difference modeling of nonlinear phenomena in time-domain electromagnetics: a review. In: Rassias T (ed) Applications of nonlinear analysis. Springer optimization and its applications, vol 134. Springer, Cham